Pauli Channel Online Estimation Protocol for Quantum Turbo Codes

Josu Etxezarreta Martinez (*Student Member, IEEE*)
Department of Basic Sciences and Bioengineering
Tecnun - University of Navarra
Donostia, Spain
jetxezarreta@tecnun.es

Patricio Fuentes (*Student Member, IEEE*)
Department of Basic Sciences and Bioengineering
Tecnun - University of Navarra
Donostia, Spain
pfuentesu@tecnun.es

Pedro M. Crespo (*Senior Member, IEEE*)
Department of Basic Sciences and Bioengineering
Tecnun - University of Navarra
Donostia, Spain
pcrespo@tecnun.es

Javier Garcia-Frías, (*Senior Member, IEEE*)
Department of Electrical and Computer Engineering
University of Delaware
Newark, USA
jgf@udel.edu

***Abstract*—In this paper, we tackle the channel estimation problem for Pauli channels. Online estimation methods for the depolarizing channel have been proposed in previous literature. However, realistic quantum devices often exhibit an asymmetric behaviour not captured by the symmetric depolarizing model, implying that the estimation method used by Quantum Turbo Codes (QTC) should exploit such asymmetry for the error correcting operations to be successful. Consequently, we propose an online iterative method that aids in successfully estimating each of the individual error probabilities associated with the Pauli channel, ultimately increasing the probability of correct decoding. The benefits this method provides come at the expense of an increase in the decoding complexity.**

***Index Terms*—quantum error correction, turbo codes, realistic devices, estimation**

I. Introduction

Quantum technologies have shown immeasurable potential to effectively solve several information processing tasks such as prime number factorization [1] or unstructured database searches [2]. Unfortunately, quantum information is susceptible to corruption given its tendency to interact with the surrounding environment. The set of interactions that corrupts the superposition states that define quantum information is known as *environmental decoherence*. Dealing with this phenomenon appropriately is pivotal to succesfully construct operational quantum devices. The stratagems that combat the deleterious effects the aforementioned noise causes on quantum states are known as Quantum Error Correction Codes (QECC). Quantum information is so sensitive to decoherence that many think that quantum computation is unfeasible without the aid of quantum error correction tools.

Quantum error correction codes have been studied and designed in the context of the depolarizing channel [3]- [8], which is the symmetric instance of the generic Pauli channel over which the probabilities of bit-flips ($\mathbf{X}$), phase-flips ($\mathbf{Z}$) and bit-and-phase-flips ($\mathbf{Y}$) are considered to be the same $p_x = p_y = p_z$. However, not all state of the art implementations of quantum hardware exhibit such an equiprobable distribution for Pauli errors [9]. Therefore, the corresponding asymmetry must be taken into account when designing error detection and correction methods. For the devices considered at the time of writing, phase-flip ($\mathbf{Z}$) errors dominate over bit-flips ($\mathbf{X}$) and bit-and-phase-flips ($\mathbf{Y}$) by several orders of magnitude, and so the asymmetry degree α of these Pauli channels is defined as the ratio of the phase-flip probability (p_z) over the bit-flip probability (p_x). This asymmetry can vary from $\alpha = 1$ to $\alpha = 10^6$ depending on the specific materials and methods used to create quantum devices [9].

Asymmetric QECCs have been studied in the literature [9] - [12] under the stringent assumption that the decoders have perfect knowledge of the asymmetric channel probabilities. However, we are not aware of any work dealing with QECCs for asymmetric channels when these probabilities are not known. For the case of the depolarizing channel, the authors in [3] were the first to propose an online channel estimation method capable of operating without the need for prior knowledge of the channel depolarizing probability.

In this article, we propose an extension of the online estimation method introduced in [3] to cover the more general case of the Pauli channel with asymmetries. The performance of the overall QECC system is tested via Monte Carlo simulations, and the results show that near-capacity performance is obtained.

The remainder of the article is organized as follows: Section II presents the general Pauli channel and the QTC considered in this paper. Section III describes the version of the online estimation method of [3] adapted to the asymmetric channel, and shows the results obtained for said methodology. Finally, Section IV presents the conclusions reached in this paper.

This work was supported by the Spanish Ministry of Economy and Competitiveness through the ADELE project (PID2019-104958RB-C44). This work has been funded in part by NSF Award CCF-2007689. Josu Etxezarreta is funded by the Basque Government predoctoral research grant.

978-1-7281-8969-7/20/$31.00 ©2020 IEEE
DOI 10.1109/QCE49297.2020.00023

II. Pauli channel and Quantum Turbo Codes

A. Pauli channel

The most popular channel considered in QECC is the so-called *depolarizing channel* $\mathcal{N}_D$ [3] - [8]. The action of this channel on an arbitrary quantum state ρ is defined as

$$\mathcal{N}_D(\rho, p) = (1-p)\rho + \frac{p}{3}(\mathbf{X}\rho\mathbf{X} + \mathbf{Y}\rho\mathbf{Y} + \mathbf{Z}\rho\mathbf{Z}), \quad (1)$$

where p is the depolarizing probability, and $\mathbf{X}, \mathbf{Y}, \mathbf{Z}$ are the Pauli matrices. However, some of the materials used to construct quantum devices behave in an asymmetric manner, where phase-flips ($\mathbf{Z}$) are orders of magnitude more likely to occur during channel operation than bit-flips ($\mathbf{X}$) and bit-and-phase-flips ($\mathbf{Y}$) [9]. The quantum channel that captures such an asymmetry is called *Pauli channel* $\mathcal{N}_P$, and its action on an arbitrary quantum state ρ is described as

$$\begin{aligned}\mathcal{N}_P(\rho, p_x, p_y, p_z) =&(1-p_x-p_y-p_z)\rho + p_x\mathbf{X}\rho\mathbf{X} \\ &+ p_y\mathbf{Y}\rho\mathbf{Y} + p_z\mathbf{Z}\rho\mathbf{Z},\end{aligned} \quad (2)$$

where p_x, p_y, p_z represent the probability that each of the possible Pauli errors occurs. These probabilities can be related to the single-qubit relaxation time T_1 and dephasing time T_2 of the quantum device under consideration as [13]

$$p_x = p_y = \frac{1 - e^{\frac{-t}{T_1}}}{4} \quad (3)$$

and

$$p_z = \frac{1 - e^{\frac{-t}{T_2}}}{2} - \frac{1 - e^{-\frac{-t}{T_1}}}{4}, \quad (4)$$

where t refers to the coherent operation duration. Since p_x and p_y are the same, it is convenient to define the following asymmetry ratio α [14]

$$\alpha = \frac{p_z}{p_x} = 1 + 2\frac{1 - e^{\frac{t}{T_1}\left(1-\frac{T_1}{T_2}\right)}}{e^{\frac{t}{T_1}} - 1}. \quad (5)$$

Using α, the expression for the Pauli channel (2) can be rewritten as

$$\begin{aligned}\mathcal{N}_P(\rho) =&(1-p)\mathbf{I}\rho\mathbf{I} + \frac{p}{\alpha+2}\mathbf{X}\rho\mathbf{X} \\ &+ \frac{p}{\alpha+2}\mathbf{Y}\rho\mathbf{Y} + \frac{\alpha p}{\alpha+2}\mathbf{Z}\rho\mathbf{Z},\end{aligned} \quad (6)$$

where $p = p_x + p_y + p_z$.

Table I shows the relaxation time T_1, dephasing time T_2 and the asymmetry coefficient for some of the quantum devices that can currently be found on the market. Note that the range of values[1] of the asymmetry coefficients is $\alpha \in [1, 10^6]$. Therefore, any online estimation method applied to aid QTCs to reach near-capacity performance should be able to cope with all these scenarios.

[1]The value diversity stems from the fact that each device uses a different technology in order to construct its qubits, i.e., superconducting qubits, trapped ions, etc.

TABLE I
Relaxation time T_1, dephasing time T_2 and asymmetry parameter α for some of the quantum devices that are currently available

Name	$\mathbf{T_1}(\mu\mathbf{s})$	$\mathbf{T_2}(\mu\mathbf{s})$	α
IBM Q System One [15]	73.9	69.1	≈ 1
Rigetti 32Q Aspen-7 [16]	41	35	≈ 1
Google Sycamore [9], [17]	≈ 1	≈ 0.1	≈ 10
Ion Q 11 Qubit [18]	$> 10^{10}$	$> 10^6$	$\approx 10^4$
Intel Q (Spin Qubits) [9], [19]	$> 10^9$	$> 10^3$	$\approx 10^6$

Observe that in the case where the coherent time duration t of a specific device is such that $t << T_1$, then α can be approximated as $\alpha \approx 2T_1/T_2 - 1$ [14]. In the present study, we assume this condition holds (i.e., we assume that the coherent time duration of the device is relatively small in comparison to the relaxation time). However, we will assume no knowledge of α in the decoding process, and the decoder will estimate its value on the fly. At first glance, it may seem unnecessary to estimate the parameter α, as it may be reasonable to assume that the decoder knows the asymmetry level of the technology being used. Nevertheless, for quantum operations that require a significant coherent time duration when compared to the relaxation time of the device, the parameter α will be a function of time and will vary, even if the technology is maintained. Moreover, the relaxation and dephasing times are dependent on the physical conditions of the device, such as temperature [20], and fluctuations of those parameters will lead to changes in the asymmetry level. As a consequence, estimating α on the fly in the decoding process is of great importance, since a mismatch between the real value of α and the one assumed at the decoder would result in substantial performance degradation.

B. Quantum Turbo Codes

The Quantum Turbo Codes considered in this paper consist of the interleaved serial concatenation of unassisted QCCs acting as outer and inner codes, following the rationale of [9]. Figure 1 presents the full schematic representation of such a quantum error correction system. The k input logical qubits that make up the information word $|\psi_1\rangle$ are first fed to the outer convolutional encoder $\mathcal{V}_1$, and encoded into n' physical qubits with the help of ancilla qubits and memory qubits. The codeword $|\bar{\psi}_1\rangle$ consists of n' physical qubits generated by the first encoder, which are then passed through a quantum interleaver Π, before being used as the input to the inner convolutional encoder $\mathcal{V}_2$. Such an encoder is an unassisted device that encodes the interleaved sequence of n' qubits $|\psi_2\rangle$ into the codeword $|\bar{\psi}_2\rangle$ of length N, aided by ancilla qubits and memory qubits. The codeword $|\bar{\psi}_2\rangle$ is then transmitted through a quantum Pauli channel with overall error probability p and asymmetry ratio α, which inflicts an N-qubit Pauli error $\mathcal{P}_2 \in \mathcal{G}_N$ on the codeword. The Pauli channel is independently applied to each of the qubits of the stream $|\bar{\psi}_2\rangle$, and, consequently, each of the qubits experiences a bit-flip ($\mathbf{X}$ operator) with probability $p_x = p/(\alpha+2)$, a phase-flip ($\mathbf{Z}$

operator) with probability $p_z = \alpha p/(\alpha+2)$ or a combination of both ($\mathbf{Y}$ operator) with probability $p_y = p/(\alpha+2)$, as described in equation (6).

At the output of the depolarizing channel, the state $\mathcal{P}_2\left|\bar{\psi}_2\right\rangle$ is fed to the inverse of the inner encoder $\mathcal{V}_2^\dagger$, which outputs the decoded state $\mathcal{L}_2\left|\psi_2\right\rangle$, where $\mathcal{L}_2 \in \mathcal{G}_{n'}$ refers to the logical error suffered by the decoded state due to the operation of the channel; and the classical syndrome bits S_2^x obtained from Z basis measurements on the ancilla qubits. The corrupted logical qubits are then passed through a de-interleaver Π^{-1} resulting in the state $\mathcal{P}_1\left|\bar{\psi}_1\right\rangle$, which is supplied to the inverse of the outer encoder $\mathcal{V}_1^\dagger$. The resulting output is the state $\mathcal{L}_1\left|\psi_1\right\rangle$, which corresponds to the information quantum state corrupted by a logical error $\mathcal{L}_1 \in \mathcal{G}_k$; and the classical syndrome bits S_1^x obtained after measuring the ancilla qubits on the Z basis. The classical syndromes S_2^x and S_1^x, obtained in the inverse decoders $\mathcal{V}_2^\dagger$ and $\mathcal{V}_1^\dagger$, respectively, are then provided to the iterative syndrome decoder made up of two serially concatenated SISO decoders, as shown in Figure 1. Based on S_2^x and S_1^x, as well as the channel depolarization probability $\mathrm{P}_{ch}(\mathcal{P}_2)$, both SISO decoders engage in degenerate iterative decoding [5], [21] to estimate the most likely error coset $\tilde{\mathcal{L}}_1$ that has corrupted the information quantum state. Based on the aforementioned estimation, a recovery operation $\mathcal{R}$ is applied to the corrupted state $\mathcal{L}_1\left|\psi_1\right\rangle$, yielding the recovered output $\left|\tilde{\psi}_1\right\rangle$.

As mentioned previously, the aim of this paper is to adapt

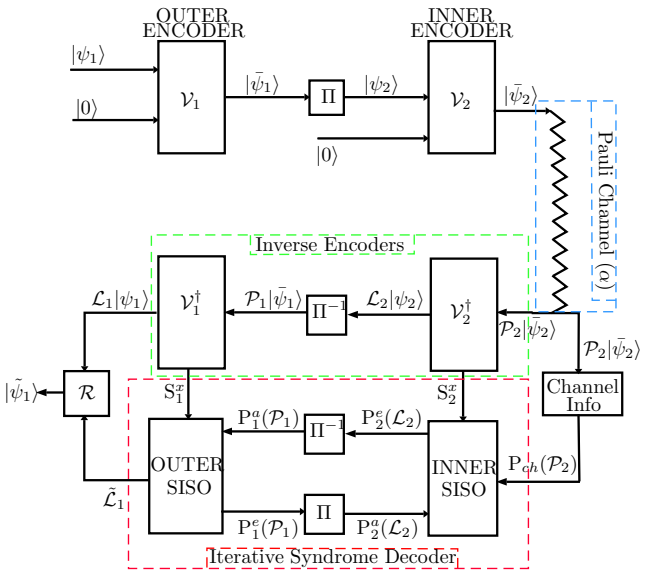

Fig. 1. Schematic of the QTC. $\mathrm{P}_i^a(.)$ and $\mathrm{P}_i^e(.)$ denote the a-priori and extrinsic probabilities related to each of the SISO decoders used for turbo decoding. The k input logical qubits that make up the information word $|\psi_1\rangle$ are first fed to the outer convolutional encoder $\mathcal{V}_1$, and encoded into n' physical qubits $|\bar{\psi}_1\rangle$ with the help of ancilla qubits and memory qubits. The codeword $|\bar{\psi}_1\rangle$ is then passed through a quantum interleaver Π, before being used as the input to the inner convolutional encoder $\mathcal{V}_2$, which aided by ancillary qubits and memory qubits encodes the interleaved sequence of n' qubits $|\psi_2\rangle$ into the codeword $|\bar{\psi}_2\rangle$ of length N.

TABLE II
NOISE LIMITS p^* FOR QUANTUM RATE $R_Q = 1/9$ AS A FUNCTION OF THE ASYMMETRY COEFFICIENT OF THE CHANNEL α.

PTO1R-PTO1R (Unassisted)				
α	1	10^2	10^4	10^6
$\mathbf{p}^*$	0.1603	0.2729	0.3056	0.3064

the online estimation system designed in [3] for the depolarizing channel to the more general asymmetric Pauli channel. With that purpose in mind, the QCCs used for the quantum turbo code in Figure 1 are the "PTO1R" unassisted convolutional encoders that were used in [9]. The seed transformation[2] associated with the convolutional encoders is

$$\begin{aligned}\mathcal{U} = \{&1355, 2847, 558, 2107, 3330, 739,\\ &2009, 286, 473, 1669, 1979, 189\}.\end{aligned} \tag{7}$$

Performing the interleaved concatenation of two of those QCCs engenders the QTCs that will be considered throughout this paper. We will refer to such a concatenated error correction scheme as the *"PTO1R-PTO1R" configuration*, following previous work in the literature. This QTC is formed by two similar QCC encoders of rate $1/3$ resulting in a rate $R_Q = R_{in} \times R_{out} = 1/3 \times 1/3 = 1/9$ error correction scheme. Additionally, the entanglement consumption of the code will be null as all the encoders are unassisted QCCs. Finally, each of the "PTO1R" encoders is aided by 3 memory qubits in order to perform the convolutional encoding operation.

This configuration was extensively studied in [6] for asymmetry values $\alpha \in \{1, 10^2, 10^4, 10^6\}$ under the assumption that channel information is known at the decoder. For that reason, we will employ it as a benchmark for this paper and we will test the configuration with the proposed estimation method for these asymmetry coefficients. The unassisted hashing bound for the Pauli channel is calculated as [9]

$$\begin{aligned}C_Q(p_x, p_y, p_z) =& 1 + (1-p)\log_2(1-p) + p_x \log_2(p_x)\\ &+ p_y \log_2(p_y) + p_z \log_2(p_z),\end{aligned} \tag{8}$$

where $p = p_x + p_y + p_z$. The asymmetry coefficient α can be used in order to rewrite (8) as

$$\begin{aligned}C_Q(p, \alpha) =& 1 + (1-p)\log_2(1-p) + \left(\frac{2p}{\alpha+2}\right)\log_2\left(\frac{p}{\alpha+2}\right)\\ &+ \left(\frac{\alpha p}{\alpha+2}\right)\log_2\left(\frac{\alpha p}{\alpha+2}\right).\end{aligned} \tag{9}$$

Using the values presented in Table I for realistic quantum devices, we can calculate the noise limit p^* for each of them by using the hashing bound in equation (9). Table II presents these noise limits for different values of the asymmetry coefficient when the quantum rate is $R_Q = 1/9$.

[2]The seed transformation $\mathcal{U}$ is represented using the decimal representation presented in [5].

III. Online estimation method for the Pauli channel

In this section, we describe the modified online estimation algorithm for the asymmetric channel. Furthermore, we present results that support the claim that the proposed method successfully achieves the task at hand.

A. Online method for the Pauli channel

The online estimation method presented in [3] for the depolarizing channel is grounded in the idea of exploiting the already available channel physical error probability distribution $\mathrm{P}^j(\mathcal{P}_2^i|\mathrm{S}_2^x)$ at each iteration j and for each i^{th} qubit when running the sum-product algorithm on the turbo decoder. In [3], it was concluded that a mismatch between the true depolarizing probability and the depolarizing probability fed to the decoder results in a degradation of the error correction capability of the QECC. Successful estimation is even more important for the general Pauli channels considered here, which depend on more parameters than depolarizing channels.

Based on these probabilities, the depolarizing parameter p can be estimated at iteration j as

$$\hat{p}^{(j)} = 1 - \frac{1}{N}\sum_{i=1}^{N} \mathrm{P}^j(\mathcal{P}_2^i = I|\mathrm{S}_2^x). \tag{10}$$

In previous works, these probabilities were left unused, and only the probabilities related to the logical error $\mathrm{P}_2^e(\mathcal{L}_2)$ associated with the inner QCC were further processed.

In the online estimation method of [3], once $\hat{p}^{(j)}$ was obtained it was fed back to the outer SISO decoder to be used in the next iteration as the *a priori* channel probability distribution. Simulation results showed that by setting $\hat{p}^{(1)}$ to the noise limit p^* for the first iteration, good performance was obtained.

For the case considered in this work, the online estimation method for the general asymmetric Pauli channel, at each iteration j the channel probabilities $\hat{p}_g^{(j)}$ with $g \in \{\mathbf{X}, \mathbf{Y}, \mathbf{Z}\}$ must be estimated. Following the same reasoning as in the depolarizing channel, we propose the following estimator:

$$\hat{p}_g^{(j)} = \frac{1}{N}\sum_{i=1}^{N} \mathrm{P}^j(\mathcal{P}_2^i = g|\mathrm{S}_2^x), \tag{11}$$

where $g \in \{\mathbf{X}, \mathbf{Y}, \mathbf{Z}\}$. Once such values are obtained, they are used to derive the *a priori* channel probability distribution $\hat{\mathrm{P}}_{ch}(\mathcal{P}_2)$, which is fed back to the inner SISO decoder for the next iteration of the turbo decoding sum-product algorithm, as reflected in figure 2.

Note that in (11), each of the probabilities associated with each of the non-identity Pauli matrices is calculated independently. One might wonder why not to use the fact that for the asymmetric channel being considered the probabilities for bit-flip and bit-and-phase-flip are equal, and thus to force the estimator to estimate $\hat{p}_x^{(j)} = \hat{p}_y^{(j)}$ by calculating the mean of both. In principle, this would lead to better performance, as information about the channel structure would be indirectly fed to the decoder. However, as it will be seen in the simulation results, the proposed decoder achieves the same performance as a decoder that has knowledge of the channel parameters. Consequently, the only benefit that might be obtained by applying such restriction in the estimation procedure would be to lower the decoding complexity. Reducing the complexity is desirable, but we consider that the method proposed in (11) is more interesting, as it will be valid for all types of Pauli channels and not just for the asymmetric model being considered in this paper.

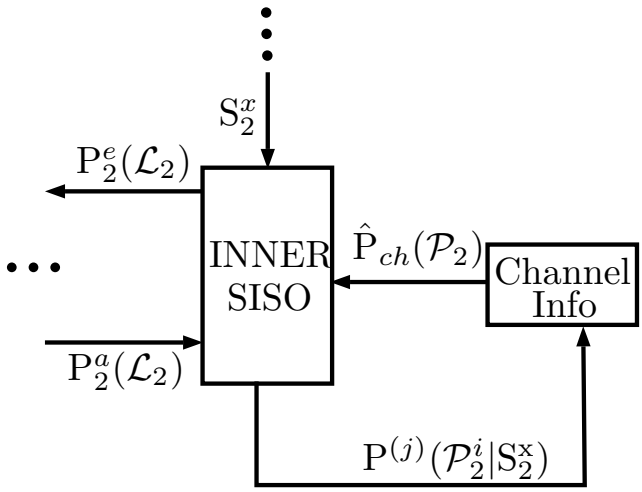

Fig. 2. Modified QTC decoder to perform online estimation of the distribution of the general Pauli channel based on the measured syndrome S_2^x. The figure only presents the inner SISO part of the decoder, as the rest of the turbo decoder remains unchanged.

The final matter that must be established in order to appropriately define the iterative online estimation algorithm is the selection of the values for the first iteration, $\hat{p}_g^{(1)}, g \in \{\mathbf{X}, \mathbf{Y}, \mathbf{Z}\}$. Following the reasoning of [3], it seems logical to select $\hat{p}_g^{(1)} = \alpha p_\alpha^*/(\alpha+2)$ for $g = \mathbf{Z}$ and $\hat{p}_g^{(1)} = p_\alpha^*/(\alpha+2)$ for $g = \{\mathbf{X}, \mathbf{Y}\}$, where p_α^* refers to the noise limit for the code with channel asymmetry α. However, the parameter α is unknown by the receiver, and so we cannot set such a starting point for the algorithm. Consequently, we will select the value for the first iteration as a constant for each g. Observing figure 10 in [3], it can be inferred that the selection of the initial values is not crucial in terms of code performance if the number of iterations for the turbo decoding algorithm is sufficient. In light of these results, and of the fact that the noise limit p_α^* increases[3] with the value of α [9], we will select the starting point of the algorithm as $\hat{p}_g^{(1)} = p_{\alpha=1}^*/3, \forall g$. The estimated asymmetry parameter for each iteration can be obtained as

$$\hat{\alpha}^{(j)} = \frac{\hat{p}_{g=Z}^{(j)}}{\hat{p}_{g=X}^{(j)}}. \tag{12}$$

[3]Since operating beyond the noise limit of a code does not make sense, it is logical to select the smallest noise limit as the starting point of all possible asymmetry coefficients α. The smallest noise limit is given by the symmetric case $\alpha = 1$ [9].

The proposed estimation method is applicable for all possible values of α.

B. Simulation Results

In this section we perform Monte Carlo simulations to asses the performance of Quantum Turbo Codes using the proposed online estimation method for asymmetric Pauli channels. For this purpose, the QTC scheme presented in section II has been used with a block length of $k = 1000$ logical qubits, as done in [9] for the system using perfect channel information.

In order to perform the numerical simulations, as in [3], [7], an N-qubit error is randomly generated in each transmission round as explained in (6). At the decoder, the syndromes S_1^x and S_2^x are computed first, and the turbo decoding algorithm runs until the hard decisions on the estimated logical errors are the same as in the previous iteration, or until the number of iterations reaches the maximum value.

The operational figure of merit selected in order to evaluate the performance of these quantum error correction schemes is the *Word Error Rate* (WER), which is the probability that at least one qubit of the received block is incorrectly decoded.

Regarding the numerical Monte Carlo methods used in order to estimate the WER of the different QTCs, the following rule of thumb has been used in order to select the number of blocks to be transmitted, N_{blocks}:

$$N_{blocks} = \frac{100}{\mathrm{WER}}. \tag{13}$$

As explained in [3], [7], under the assumption that the observed error events are independent, this results in a 95% confidence interval of about $(0.8\hat{\mathrm{WER}}, 1.25\hat{\mathrm{WER}})$, where $\hat{\mathrm{WER}}$ refers to the empirically estimated value for the WER.

Figure 3 shows the results obtained for the QTCs described in section II using the generalized online estimation method presented in section III-A. The waterfall shaped curves depicted in said figure compare the performance of the "PTO1R-PTO1R" configuration when it corrects errors of asymmetric nature and its decoder has access to perfect channel information, to the performance of the decoder that estimates those channel parameters while simultaneously decoding the information. It is obvious that both methods exhibit similar error correcting capabilities in terms of WER performance. Consequently, the generalized online estimation method allows the QTCs to attain excellent performance regardless of the nature of the channel. This outcome is of significant relevance, since it means that the QTC decoder can be applied to any Pauli channel. Therefore, no channel-specific QTC decoders that need to know the exact noise model beforehand are required.

To finalize the study of the QTCs that use the online estimator to tackle the lack of knowledge about the channel parameters, we discuss the number of iterations required by the turbo decoder algorithm to succesfully estimate the logical error coset. In [9], the authors claim that setting the maximum number of iterations beyond $I_{max} = 4$ produced no benefits in the decoding process. However, the utilization of the online method introduced in our work requires the decoder to execute more iterations so that the recovery operation can be calculated correctly. This need arises because the decoder estimates the channel parameters during every decoding iteration, which inadvertently implies that subsequent estimates become increasingly accurate as more decoding rounds take place. Thus, the decoder requires sufficient iterations for the channel information to be accurate enough to produce satisfactory estimates of the logical error coset through additional turbo decoder rounds. For the codes considered in this article, we have observed that setting the maximum number of iterations to less than $I_{max} = 32$ implies a loss in the WER performance, while increasing the parameter beyond this value yields no benefit for the QTCs under consideration. As a result, the worst case decoding scenario using our estimator takes 8 times the number of decoding rounds required by a decoder that has knowledge of the channel parameters. However, the increase in complexity is justified by the flexibility provided by the online estimation method, since if we assume that the channel remains constant for the duration of the block, the QTC performance will not be compromised if the nature of the channel changes from block to block, regardless of whether the change occurs in the gross error probability p or in the asymmetry level of the Pauli channel α. Therefore, QTCs will achieve excellent performance independently of the nature of the channel or its time evolution.

Another question that comes up when analyzing the performance of the proposed online asymmetry-considering estimator is how it measures up against the online estimator proposed in [3]. The answer to this question will give us information regarding the importance of asymmetry to decode QTCs. Figure 4 shows the results obtained by running the turbo decoder with the estimator from [3], as well as the results obtained for the extended online estimator proposed in this paper, when we consider the Pauli channels with asymmetry coefficients $\alpha = 10^2$ and $\alpha = 10^6$. Notice that neglecting the possibility that the channel might be asymmetric and treating it like a depolarizing channel leads to huge performance losses. Upon further examination of figure 4, it can be seen that using the estimator from [3] for the Pauli channel always results, independently of the nature of α, in the QTC performance corresponding to the symmetric case $\alpha = 1$. As a consequence, if asymmetry is not considered in the error correction system, the performance loss experienced by the QTCs will correspond to the distance between the waterfall region presented by the decoder that has perfect knowledge of the channel parameters and the waterfall region of the decoder for the depolarizing channel, which increases with the growth of the asymmetry coefficient α. In practical situations, since the quantum channel might be asymmetric, using the extended online estimator proposed in this paper is paramount if one wants to maintain excellent performance.

IV. Conclusions

We have presented an extension of an existing online estimation method for the depolarizing channel, making it

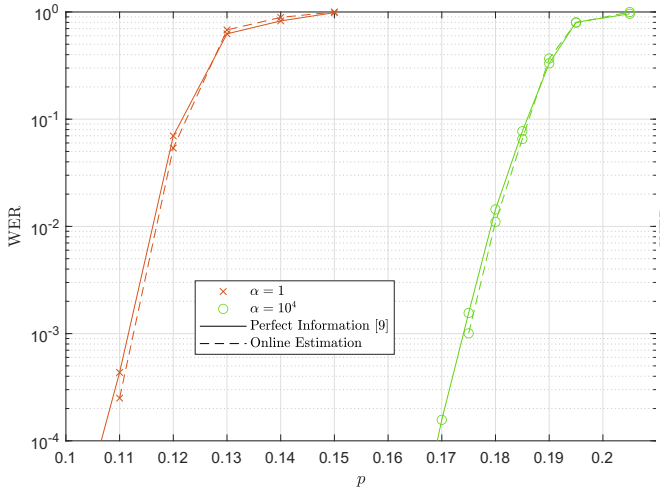

(a) WER performance of the QTC for $\alpha = 1$ and $\alpha = 10^4$.

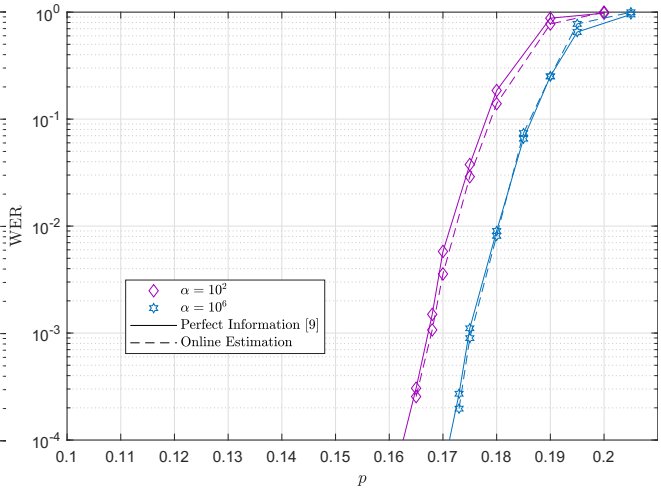

(b) WER performance of the QTC for $\alpha = 10^2$ and $\alpha = 10^6$.

Fig. 3. WER performance for the QTC under consideration when the proposed online estimation procedure is utilized with initial value $\hat{p}_g^{(1)} = p^*_{\alpha=1}/3 = 0.1603/3, \forall g \in \{\mathbf{X}, \mathbf{Y}, \mathbf{Z}\}$. The obtained performance curves are compared to the ones obtained in [9] for the case where the QTC decoders have knowledge of the parameters p and α.

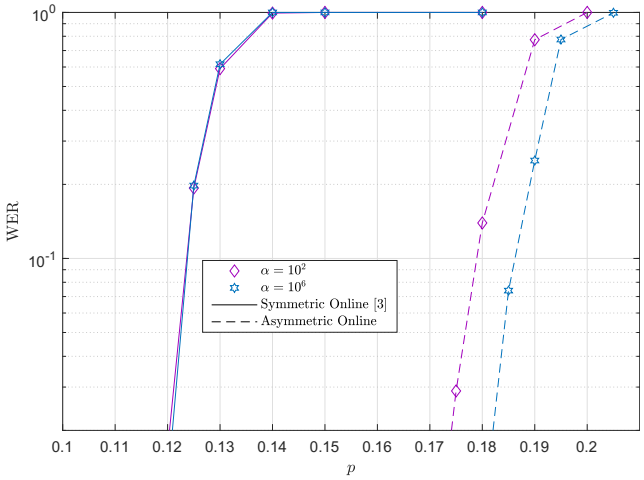

Fig. 4. WER performance of the QTCs using the symmetric online estimator from [3] against the performance of those QTCs using the online asymmetric estimator proposed in the present article. The considered asymmetry coefficients are $\alpha = 10^2$ and $\alpha = 10^6$.

capable of considering the asymmetries that are present in the decoherence models of realistic quantum devices. The noise in these devices is modeled using the well known Pauli channel, which has been shown to be biased towards $\mathbf{Z}$ type errors for some of the qubit construction technologies that are being used in this day and age. As a consequence, the existing estimation methods fail to perform appropriately for technologies used in the construction of quantum devices.

Our proposed extended method uses the information that is processed in each iteration of the sum-product decoder to estimate each probability of the asymmetric channel individually. Monte Carlo simulations corroborate that the proposed online estimation method is successful in aiding the QTC to achieve the same performance as when it has access to the channel parameters. This positive outcome comes at the cost of a slight increase in the complexity of the decoding algorithm. However, the flexibility that the proposed method provides, allowing the QTCs to be able to operate close to their hashing bounds without requiring any knowledge of the Pauli channel parameters or of how they evolve in time, far outweighs this minor drawback.

REFERENCES

[1] P. W. Shor, "Polynomial-Time Algorithms for Prime Factorization and Discrete Logarithms on a Quantum Computer," *SIAM Journal on Computing*, vol. 26, no. 5, pp. 1484–1509, 1997.

[2] L. K. Grover, "A Fast Quantum Mechanical Algorithm for Database Search," *Annual ACM Symp. on Theory of Comp.*, pp. 212–219, 1996.

[3] J. Etxezarreta Martinez, P. Crespo, and J. Garcia-Frías, "Depolarizing Channel Mismatch and Estimation Protocols for Quantum Turbo Codes", *Entropy*, 21, 1133, 2019.

[4] D. Poulin, J. Tillich, and H. Ollivier, "Quantum serial turbo codes", *IEEE Trans. Inf. Theory*, 55, 2776-2798, 2009.

[5] M. Wilde, M. Hsieh, and Z. Babar, "Entanglement-Assisted Quantum Turbo Codes", *IEEE Trans. Inf. Theory*, 60, 1203–1222, 2014.

[6] Z. Babar, S.X. Ng, and L. Hanzo, "EXIT-Chart-Aided Near-Capacity Quantum Turbo Code Design", *IEEE Trans. Vech. Technol.*, 64, 866–875, 2015.

[7] J. Etxezarreta Martinez, P. Crespo, and J. Garcia-Frías, "On the Performance of Interleavers for Quantum Turbo Codes", *Entropy*, 21, 633, 2019.

[8] Z. Babar, P. Botsinis,D. Alanis, S.X. Ng, and L. Hanzo, "Fifteen Years of Quantum LDPC Coding and Improved Decoding Strategies", *Access IEEE*, 3, 2492-2519, 2015.

[9] H.V. Nguyen, Z. Babar, D. Alanis, P. Botsinis, D. Chandra S.X. Ng, and L. Hanzo, "EXIT-Chart Aided Quantum Code Design Improves the Normalised Throughput of Realistic Quantum Devices", *Access IEEE*, 4, 10194-10209, 2016.

[10] L. Loffe, and M. Mézard, "Asymmetric quantum error-correcting codes", *Phys. Rev. A*, 75(3), 032345, 2007.

[11] L. Wang, K. Feng, S. Ling, and C. Xing, "Asymmetric quantum codes: Characterization and constructions", *IEEE Trans. Inf. Theory*, 56(6), 2938–2945, 2010.

[12] G. La Guardia, "On the construction of asymmetric quantum codes", *Int. J. Theor. Phys.*, 53(7), 2312–2322, 2014.
[13] J. Ghosh, A.G. Fowler, and M.R. Geller, "Surface code with decoherence: An analysis of three superconducting architectures", *Phys. Rev. A*, 86, 062318, 2012.
[14] P.K. Sarvepalli, P. Klappenecker, and M. Röteller, "Asymmetric quantum codes: constructions, bounds and performance", *Proc. R. Soc. A*, 465, 1645-1672, 2009.
[15] J. Gambetta, and S. Sheldon, "Cramming More Power Into a Quantum Device", *IBM*, March 4, 2019. Accessed on: May 22, 2020. [Online]. Available: https://www.ibm.com/blogs/research/2019/03/power-quantum-device/.
[16] Amazon Braket, "Amazon Braket Hardware Providers", *Amazon Web Services*, October 24, 2019. Accessed on: May 22, 2020. [Online]. Available: https://aws.amazon.com/braket/hardware-providers/.
[17] F. Arute, K. Arya, R. Babbush *et al.*, "Quantum supremacy using a programmable superconducting processor", *Nature*, 574, 505-510, 2019.
[18] K. Wright, K.M. Beck, S. Debnath *et al.*, "Benchmarking an 11-qubit quantum computer", *Nat. Commun.*, 10, 5464, 2019.
[19] Intel, "Reinventing Data Processing with Quantum Computing", *Intel*. Accessed on: May 22, 2020. [Online]. Available: https://www.intel.com/content/www/us/en/research/quantum-computing.html.
[20] Z. Wang, S. Shankar, Z.K. Minev, P. Campagne-Ibarcq, A. Narla, and M.H. Devoret, "Cavity Attenuators for Superconducting Qubits", *Phys. Rev. Applied*, 11, 014031, 2019.
[21] D. Poulin, J. Tillich, and H. Ollivier, "Quantum Serial Turbo Codes", *IEEE Trans. Inf. Theory*, 55(6), 2776-2798, 2009.